

# Computer Study of Cluster Mechanism of Anti-greenhouse Effect

A. Galashev

**Abstract**—Absorption spectra of infra-red (IR) radiation of the disperse water medium absorbing the most important greenhouse gases:  $\text{CO}_2$ ,  $\text{N}_2\text{O}$ ,  $\text{CH}_4$ ,  $\text{C}_2\text{H}_2$ ,  $\text{C}_2\text{H}_6$  have been calculated by the molecular dynamics method. Loss of the absorbing ability at the formation of clusters due to a reduction of the number of centers interacting with IR radiation, results in an anti-greenhouse effect. Absorption of  $\text{O}_3$  molecules by the  $(\text{H}_2\text{O})_{50}$  cluster is investigated at its interaction with  $\text{Cl}^-$  ions. The splitting of ozone molecule on atoms near to cluster surface was observed. Interaction of water cluster with  $\text{Cl}^-$  ions causes the increase of integrated intensity of emission spectra of IR radiation, and also essential reduction of the similar characteristic of Raman spectrum. Relative integrated intensity of absorption of IR radiation for small water clusters was designed. Dependences of the quantity of weight on altitude for vapor of monomers, clusters, droplets, crystals and mass of all moisture were determined. The anti-greenhouse effect of clusters was defined as the difference of increases of average global temperature of the Earth, caused by absorption of IR radiation by free water molecules forming clusters, and absorption of clusters themselves. The greenhouse effect caused by clusters makes 0.53 K, and the anti-greenhouse one is equal to 1.14 K. The increase of concentration of  $\text{CO}_2$  in the atmosphere does not always correlate with the amplification of greenhouse effect.

**Keywords**—Greenhouse gases, infrared absorption and Raman spectra, molecular dynamics method, water clusters.

## I. INTRODUCTION

THE ability of the atmosphere to capture and recycle energy emitted by the Earth's surface is the defining characteristic of the greenhouse effect. Greenhouse gases dissipate heat in the atmosphere. The greenhouse effect is observed only when radiant heat stays in the troposphere, instead of leaving into Space. Layers lying above the troposphere, such as stratosphere and thermosphere, serve as an obstacle for heat loss into Space. An important role in this process belongs to the ozone layer of the bottom stratosphere and ions of oxygen in the thermosphere. The depletion of the ozone layer results in a reduction of its stabilizing function. Flight of rockets and reactive chlorine and bromine compounds render strong influence on ozone depletion and reduction of concentration of oxygen ions in the thermosphere. During the burning of atomic oxygen and

ozone, absorption of sunlight in the top layers of the atmosphere decreases. Besides the combustion, other by-products include chlorine which under certain conditions reacts with ozone and destroys it. Water, carbon and nitrogen oxides, aluminum oxide, hydrogen chloride and hydrogen are also products of rocket fuel combustion. At low temperatures, characteristic of stratosphere and the lower thermosphere, water clusters, capable of absorbing molecules of other gases are formed. Carbon dioxide is the most widespread greenhouse gas after water vapor. Molecules of carbon dioxide effectively re-emit absorbed energy. The biggest part of emitted energy leaves into the Space through ozone holes, i.e. carbon dioxide turns from greenhouse gas into anti-greenhouse one. It is probable, that observed growth of  $\text{CO}_2$  concentration in the atmosphere is a result of ozone depletion and reduction of oxygen ions concentration in the thermosphere. Then at the current rate of changes of atmosphere composition the increase of  $\text{CO}_2$  concentration will operate as a factor lowering the temperature of the planet. The potential radiative impact of the ozone change on the stratosphere-troposphere exchange was investigated in [1]. This analysis shows that a 15% global  $\text{O}_3$  decrease can cause a maximum cooling of 2.4 K in the stratosphere.

The Earth's atmosphere is a complex dynamic system, which protects the biosphere. One of the significant factors impacting the Earth's radiation balance is the greenhouse effect. Water vapor and atmospheric gases, such as  $\text{CO}_2$ ,  $\text{CH}_4$ ,  $\text{N}_2\text{O}$ , and others, have a decisive influence on the formation of thermal radiation fields. However, according to the Le Chatelier principle, there are opposite compensating processes in the atmosphere. Clusterization of greenhouse gases can be considered as one of these processes. Water molecules bind easily to one another by forming hydrogen bond complexes – clusters. These weak interactions (approximately 0.21 eV) perturb the rovibronic and electronic states of individual molecules, and alter the spectroscopy of water vapor [2]. The possible involvement of water clusters in these processes has been proposed for a long time [3–8]. The abundance and the vibrational spectrum of the water dimer and trimer were evaluated both theoretically [9] and in an experiment [10]. The temperature contributions of the greenhouse gases of the Earth's atmosphere to the greenhouse effect are determined in [11] according to their volume fraction. So for water vapor this contribution should make 37.4 K. However, correction of 13.4 K is necessary to take into account the effect of water evaporation. Therefore effectively the contribution of water vapor decreases to 24.0 K.

Y. Galashev is with the Institute of Industrial Ecology, Yekaterinburg, GSP-594, Sofia Kovalevskaya Str. 20-a, 620219 Russia (corresponding author to provide phone: +7-343-3623267; fax: +7-343-3743771; e-mail: galashev@ecko.uran.ru).

This work was supported by the Russian Foundation for Basic Research, project no. 08-08-00136.

The autoregulation of the atmosphere composition is due to the formation of water clusters and their subsequent capture of greenhouse gas molecules is, as a rule, ignored in the estimation of the Earth's radiation balance. The characteristics of infrared (IR) radiation absorption by water clusters incorporating molecules of the most abundant atmospheric gases – nitrogen, oxygen, and argon – were studied in [12–15].

The goal of this work was to establish the role of water clusters in thermal balance of atmosphere, and also to define their influence on depletion of the ozone layer.

## II. COMPUTER MODEL

This work deals with the molecular dynamics study of the influence of clusterization of H<sub>2</sub>O vapor and atmospheric gases such as CO<sub>2</sub>, N<sub>2</sub>O, CH<sub>4</sub>, C<sub>2</sub>H<sub>2</sub>, and C<sub>2</sub>H<sub>6</sub> on the greenhouse effect. The IR absorption spectra were calculated for systems formed by water clusters and molecules of the above greenhouse gases at 233 K. Due to clusterization a homogeneous single-phase system represented by a mixture of gases transforms into a "two-phase" or even "three-phase" state since, depending on the ambient conditions, clusters constituting a fine "phase" can be in both the liquid and solid states.

Water clusters were simulated using the improved interaction potential TIP4P for water and the rigid four-site model of H<sub>2</sub>O molecules [16]. The model supposes calculation of induced dipole moments of molecules, which allows inclusion for viewing of their polarization effect. The description of greenhouse gases molecules interaction with water and also between themselves is based on an atom - atom potential calculated in the Gordon-Kim approximation with the application of spherical average of electronic densities [17], [18]. To determine the influence of absorbed polyatomic molecules on the greenhouse effect, we considered different types of ultradisperse systems: (H<sub>2</sub>O)<sub>n</sub> (I), (CO<sub>2</sub>)<sub>i</sub>(H<sub>2</sub>O)<sub>10</sub> (II), (CH<sub>4</sub>)<sub>i</sub>(H<sub>2</sub>O)<sub>10</sub> (III), (N<sub>2</sub>O)<sub>i</sub>(H<sub>2</sub>O)<sub>10</sub> (IV), (C<sub>2</sub>H<sub>2</sub>)<sub>m</sub>(H<sub>2</sub>O)<sub>20</sub> (V), and (C<sub>2</sub>H<sub>6</sub>)<sub>m</sub>(H<sub>2</sub>O)<sub>20</sub> (VI), where  $n = 10-20$ ,  $i = 1-10$ , and  $m = 1-6$ . First, the molecular dynamic calculation for water clusters was carried out. The final water cluster configuration was further used as the initial configuration for heteroclusters' modeling. In the initial state the joined molecules were placed so that the minimum distance between atoms of admixture molecule and atoms of water molecules, forming a cluster, were about 0.6–0.7 nm. All considered interactions were cut off at distance of 0.9 nm. The added linear CO<sub>2</sub>, N<sub>2</sub>O and C<sub>2</sub>H<sub>2</sub> molecules were placed along the beams, connecting (H<sub>2</sub>O)<sub>10</sub> cluster's center of the mass to those of these molecules. At first CH<sub>4</sub> and C<sub>2</sub>H<sub>6</sub> molecules were placed in the knots of imaginary BCC lattice piercing the cluster. In all cases the admixture molecules were situated outside the cluster.

The Geer method of fourth order was used for the integration of the motion equations of the molecules' centers of the mass [19]. The analytical solution of motion equations for molecules' rotation was carried out with a help of the Rodrigues - Hamilton parameters [20]. Scheme of the

equations of motion integration at presence of rotation corresponded with the approach offered by Sonnenschein [21]. The duration of calculation for each cluster lasted not less than  $3 \cdot 10^6 \Delta t$ , where time step was  $\Delta t = 10^{-17}$  c.

The calculation of the autocorrelation function of the total dipole moment  $\mathbf{M}$  of the clusters makes it possible to determine their IR spectra, which characterizes absorption coefficients [22]. The IR radiation absorption cross section was specified by the equation [23]

$$\sigma(\omega) = \left( \frac{2}{\varepsilon_v c \hbar n} \right) \omega \tanh \left( \frac{\hbar \omega}{2kT} \right) \cdot \text{Re} \int_0^{\infty} dt e^{i\omega t} \langle \mathbf{M}(t) \mathbf{M}(0) \rangle, \quad (1)$$

where  $\varepsilon_v$  is the electric constant,  $c$  is the speed of light,  $\hbar = h / 2\pi$ ,  $h$  is Planck's constant, and  $n$  is the refractive index independent of the frequency  $\omega$ .

The frequency dispersion of permittivity defines the frequency dependence of dielectric loss  $P(\omega)$  in accordance with expression [24]

$$P = \frac{\varepsilon'' \langle E^2 \rangle \omega}{4\pi}, \quad (2)$$

where  $\langle E^2 \rangle$  is the average value of square of electric field intensity, and  $\omega$  is the frequency of emitted electromagnetic wave.

In displaying the depolarized Raman spectrum, we use following representation  $J(\omega)$  [23]

$$J(\omega) = \frac{\omega}{(\omega_L - \omega)^4} \left( 1 - e^{-\hbar\omega/kT} \right) \cdot \text{Re} \int_0^{\infty} dt e^{i\omega t} \langle \Pi_{xz}(t) \Pi_{xz}(0) \rangle, \quad (3)$$

$$\cdot \text{Re} \int_0^{\infty} dt e^{i\omega t} \langle \Pi_{xz}(t) \Pi_{xz}(0) \rangle,$$

where

$$\Pi(t) \equiv \sum_{j=1}^N \left[ \mathbf{p}_j(t) - \langle \mathbf{p}_j \rangle \right], \quad (4)$$

$\omega_L$  is the frequency of exiting laser,  $p_j$  is the polarizability of molecule  $j$ .

Let us consider scattering of unpolarized light when the free path  $l$  of molecules is much shorter than the light wavelength  $\lambda$ . The extinction coefficient  $\eta$  of the incident beam is determined by the Rayleigh formula [25], on one hand, and through scattering coefficient  $\rho$  ( $\eta = 16\pi\rho/3$ ) [24] assuming scattering at an angle of 90°, on another hand. Taking into account that  $\eta = \alpha + \rho$  ( $\alpha$  is the absorption coefficient), we have

$$N = \frac{2\omega^4}{3\pi^4} \frac{(\sqrt{\varepsilon} - 1)^2}{\alpha} \left(1 - \frac{3}{16\pi}\right), \quad (5)$$

where  $N$  is the number of scattering centers in  $1 \text{ cm}^3$ ,  $\varepsilon$  is the permittivity of a medium, and  $\omega$  is the incident wave frequency.

Cluster systems II-VI were formed in such a way that a cluster containing  $i$  impurity molecules had the statistical weight

$$W_i = \frac{N_i}{N_\Sigma}, \quad i=1\dots 10(6), \quad (6)$$

where  $N_i$  is the number of clusters with  $i$  impurity molecules

in  $1 \text{ cm}^3$  and  $N_\Sigma = \sum_{i=1}^{10(6)} N_i$ . Analogous weights  $W_i$  were used

for  $(\text{H}_2\text{O})_n$  clusters forming system I. All spectral characteristics were calculated using these statistical weights  $W_i$ . The procedure of cluster formation provided their uniform distribution and low concentration so that they did not interact with one another. The average concentration of each type of cluster in the systems under consideration was 12–13 orders of magnitude lower than the Loschmidt number. The rigid model of molecules used in this work does not permit consideration of intramolecular vibrations, which, as a rule, have frequencies  $\omega > 1200 \text{ cm}^{-1}$ . In this work, we study the frequency range  $0 < \omega < 1200 \text{ cm}^{-1}$ , which characterizes vibrational and rotational motions of molecules.

### III. WATER CLUSTERS AND GREENHOUSE GASES ABSORPTION

The equimolecular heterocluster  $(\text{CO}_2)_{10}(\text{H}_2\text{O})_{10}$  (Fig. 1) has a significantly irregular structure. The  $\text{CO}_2$  molecules are mixed with the  $\text{H}_2\text{O}$  molecules so that there is a correlation in their orientation. The calculated IR spectra of systems I-VI are shown in Fig. 2.

The spectra of the ultradisperse system of pure water have two peaks, the major one being at  $\omega = 974 \text{ cm}^{-1}$  (I). At the same time, the IR spectra of aqueous systems containing  $\text{CO}_2$  and  $\text{C}_2\text{H}_6$  molecules have a peak (at  $960$  (II) and  $920 \text{ cm}^{-1}$  (VI)) and a shoulder. When the cluster systems contain  $\text{CH}_4$ ,  $\text{N}_2\text{O}$ , and  $\text{C}_2\text{H}_2$  molecules, their IR spectra have a peak at  $340$  (III),  $911$  (IV), and  $920 \text{ cm}^{-1}$  (V), respectively. In the frequency range under consideration, the integrated intensity of the IR radiation absorption by systems II, III, and V is noticeably lower and that of systems IV and VI is slightly higher than the corresponding characteristic of system I.

The spectrum  $\sigma(\omega)$  of the Earth's thermal radiation, along with the experimental IR absorption spectra of liquid water and  $\text{CO}_2$ ,  $\text{CH}_4$ ,  $\text{N}_2\text{O}$ ,  $\text{C}_2\text{H}_2$ , and  $\text{C}_2\text{H}_6$  gases, is shown in the inset of Fig. 2. The water spectrum covers almost the

entire frequency range of the Earth's radiation and demonstrates the greatest contribution of atmospheric moisture to the greenhouse effect. In the frequency range studied, the positions of the major spectral peaks of gaseous  $\text{N}_2\text{O}$  and  $\text{CH}_4$  coincide. These characteristics serve as a reference for monitoring the change in the positions of the corresponding peaks in the IR spectra in going from pure water clusters to heteroclusters.

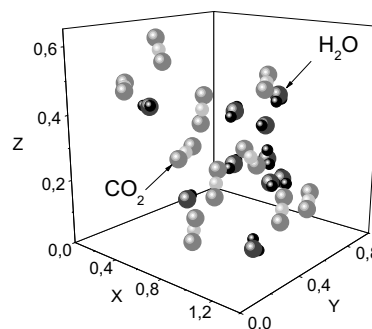


Fig. 1 Configuration of the  $(\text{CO}_2)_{10}(\text{H}_2\text{O})_{10}$  cluster at the time moment 30 ps. The coordinates of molecules are given in nanometers.

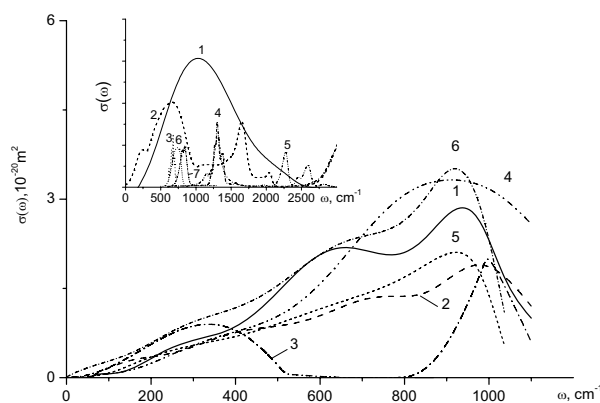


Fig. 2 IR absorption spectra of systems (1) I, (2) II, (3) III, (4) IV, (5) V, and (6) VI. In the inset: (1) the Earth's thermal radiation spectrum at  $T = 280 \text{ K}$ ; (2-7) the experimental spectra of liquid water [26] and gaseous  $\text{CO}_2$  [27],  $\text{N}_2\text{O}$ ,  $\text{CH}_4$ ,  $\text{C}_2\text{H}_2$ , and  $\text{C}_2\text{H}_6$  [28], respectively.

The anti-greenhouse effect can be developed due to a decrease in the number of absorbing centers upon the formation of water clusters. Figure 3a (curve 1) shows the relative change in the integrated IR absorption intensity  $I_{tot}$  upon the formation of the  $(\text{H}_2\text{O})_{20}$  cluster by means of successive addition of  $\Delta n$  water molecules to the  $(\text{H}_2\text{O})_2$  dimer. Curve 2 reflects the total relative intensity of the IR radiation absorption by the  $(\text{H}_2\text{O})_{10}$  cluster and five successively added dimers, which combine to produce the  $(\text{H}_2\text{O})_{20}$  cluster.

In the case of water, the formation of the cluster leads to a twofold reduction in the greenhouse effect. The major

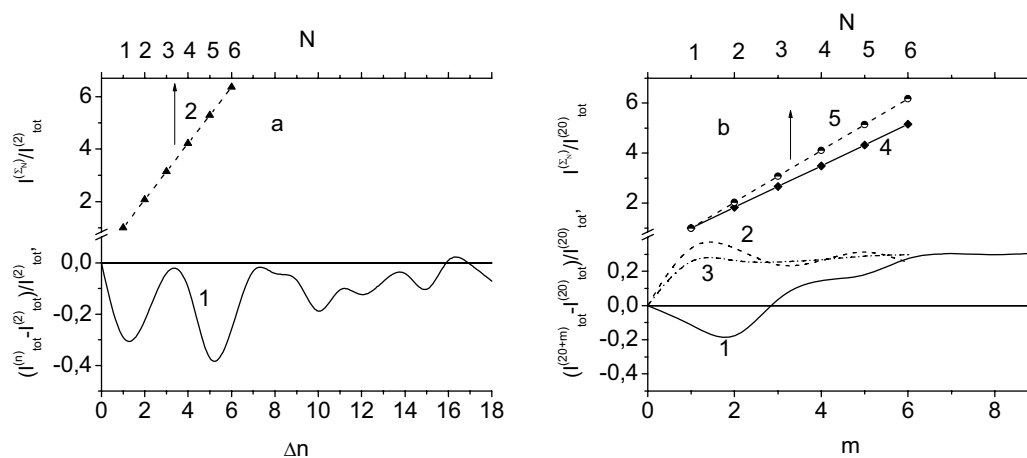


Fig. 3 (a) Relative integrated intensity of the IR absorption by (1) the water dimer that grows by adding  $\Delta n$   $H_2O$  molecules and (2) total relative integrated intensity of absorption of  $N$  clusters:  $N_1$  is  $(H_2O)_{10}$  and  $N_2 - N_6$  are  $(H_2O)_2$  dimers; (b) relative integrated intensity of the IR absorption by the  $(H_2O)_{20}$  cluster adding  $m$  molecules of (1)  $CH_4$ , (2)  $C_2H_2$  and (3)  $C_2H_6$  and total relative integrated intensity of absorption of  $N$  clusters: (4)  $N_1$  is  $(CH_4)_8(H_2O)_{10}$  and  $N_2 - N_6$  are  $(H_2O)_2$  dimers; (5)  $N_1$  is  $(CH_4)_3(H_2O)_{10}$  and  $N_2 - N_6$  are  $CH_4(H_2O)_2$  clusters.

contribution to the anti-greenhouse effect is made by the decrease in the number of absorbing centers. In addition, the buildup of the water cluster is accompanied by a decrease in its absorption capacity (curve 1 is in the range of negative values almost everywhere) due to a change in the frequency and amplitude characteristics of the total dipole moment.

The introduction of hydrocarbon molecules can enhance the IR absorption by growing clusters (Fig. 3b). The increase in  $I_{tot}$  for water cluster combined with  $C_2H_2$  and  $C_2H_6$  molecules is 0.2-0.4 of the  $I_{tot}$  value even at  $m > 1$ , whereas, when water cluster is combined with  $CH_4$  molecules, such  $I_{tot}$  values are achieved at  $m > 6$ . When one or two  $CH_4$  molecules are added to the  $(H_2O)_{20}$  cluster, the anti-greenhouse effect is enhanced since the relative integrated intensity of the IR absorption by the heterocluster decreases. However, finally, the incorporation of hydrocarbon molecules in the water clusters reduces the greenhouse effect due to a decrease in the number of absorbing centers. The anti-greenhouse effect caused by clustering is tens of times stronger than the effect due to a change in the characteristics of vibrations of the total dipole moment of clusters caused by absorption of greenhouse gas molecules. Thus, the incorporation of molecules of greenhouse gases, such as  $CO_2$ ,  $N_2O$ , and hydrocarbons  $CH_4$ ,  $C_2H_2$ , and  $C_2H_6$ , which also have an impact on the greenhouse effect, in water clusters was studied by the molecular dynamics method. The absorption of IR radiation by a disperse water system insignificantly increases when it incorporates  $N_2O$  and  $C_2H_6$  molecules and decreases when  $CO_2$ ,  $CH_4$ , and  $C_2H_2$  molecules are incorporated. When methane molecules are incorporated in water clusters, the system becomes IR transparent. Formation of water clusters and subsequent

incorporation of greenhouse gases in these clusters are accompanied by a decrease in the number of absorbing centers. Remarkably, the Earth's surface receives on average more radiation from the atmosphere and clouds than direct radiation from the Sun. On the whole, the absorption of greenhouse gases by the disperse water system results in the anti-greenhouse effect. This effect is latent because it can be defined in comparison with situation when clusters are absent. It appears that the same number of free molecules absorbs IR radiation more powerfully than when they are incorporated in a cluster.

#### IV. DESTRUCTION OF OZONE BY CHLORINE IONS ON SURFACE OF WATER CLUSTER

Let's consider ability of water clusters to absorb ozone molecules at the presence of  $Cl^-$  ions. Four runs were executed for water cluster, consisting of 50 molecules to which at the initial time moment of  $(t=0)$  6 molecules of ozone were added, and the number of chlorine ions was 0, 2, 4 and 6. At the moment of time of  $t=0$   $O_3$  molecules were at a distance of 0.5-0.6 nm from water molecules in vicinity of the lower part of the cluster (as shown in fig. 4a). The  $Cl^-$  ions influencing system, were also concentrated on one side of the cluster at a distance of 0.6-0.7 nm from molecules of water and ozone. The nearest distance between ions was about 0.9 nm. The interaction between ions, as well as interaction between ions and molecules had coulomb and polarization contributions, and also contributions from the atom-atom interaction, determined according to works [7, 8]. Configurations of the system excited by six  $Cl^-$  ions, at time moments of 0, 1.8, 3.4 and 4.4 ps are shown in fig. 4. Chlorine ions move towards water cluster due to coulomb (from hydrogen atoms of surface molecules) and polarization

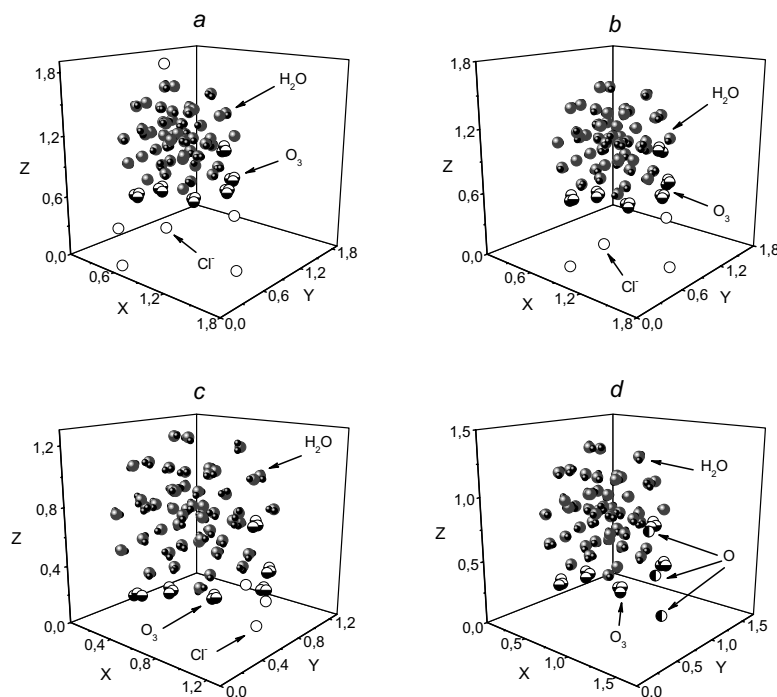


Fig. 4 Configurations of the  $(O_3)_6(H_2O)_{50} + 6 Cl^-$  system at the time moments:  $a - 0, b - 1.8, c - 3.4$  and  $d - 4.4$  ps accordingly. Coordinates of molecules are given in nanometers.

interaction, and also electrostatic repulsion from other  $Cl^-$  ions. They collide with water molecules, and receive significant kinetic energy. And then ions quickly start to leave the cluster. Thus one of  $Cl^-$  ions strongly collides with a  $O_3$  molecule which takes place near to the cluster's surface. The energy impact of this interaction exceeds the threshold value of energy  $U_{th}$  ( $=1.3$  eV), that results in splitting of ozone molecule into atoms. There is one ion in the system at the time  $t = 4$  ps, and at the moment 4.4 ps – any number of ions. The composition of the formed cluster remains constant during the rest of the time of calculation (15.6 ps).

The interaction with  $Cl^-$  ions results in essential change of Raman spectra of this cluster (fig. 5). So the integrated intensities of the  $J(\omega)$  spectrum for systems  $6O_3 + (H_2O)_{50}$  with 0, 2, 4 and 6  $Cl^-$  ions correlate as 29.7 : 4.9 : 2.6 : 1. For three last systems only two peaks located at 26 and  $511\text{ cm}^{-1}$  in the interval  $0 \leq \omega \leq 1000\text{ cm}^{-1}$  are distinct. The curve 5 in fig. 5 corresponds to the experimental Raman spectrum of liquid water obtained at premise of pure water in a tube from quartz glass, and excitation of the sample by light with a wave length of 514.5 nm [29]. Raman spectrum of liquid water has low-frequency peaks at  $\omega = 60$  and  $-30\text{ cm}^{-1}$ , and also a peak close to  $170\text{ cm}^{-1}$ . The  $60\text{ cm}^{-1}$  peak results from the bending of the hydrogen bonds between water molecules, and the  $170\text{ cm}^{-1}$  peak is due to the stretching of hydrogen bonds [23]. Stokes and anti-Stokes ranges in this spectrum are asymmetrical due to effect of photoluminescence. In a computer model such an effect is

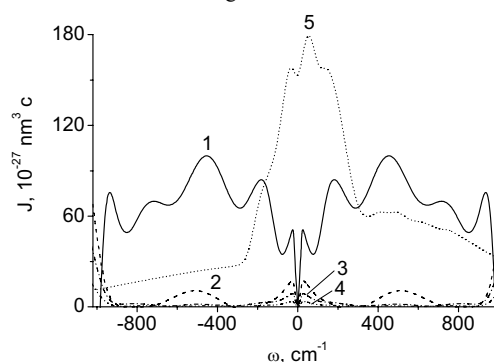


Fig. 5 Raman spectra of systems at interaction with: 1 - 0, 2-2, 3-4, 4-6  $Cl^-$  ions; 5 - liquid water, experiment [29].

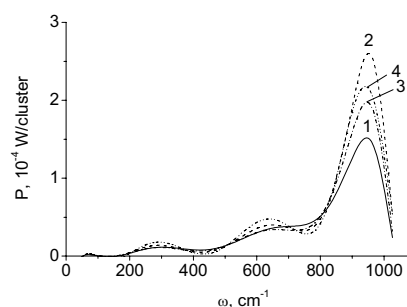


Fig. 6 Emission spectra of IR radiation by the  $(O_3)_6(H_2O)_{50}$  cluster: 1 - in absence of  $Cl^-$  ions and at interaction with: 2 - two, 3 - four, 4 - six  $Cl^-$  ions.

absent. The intensity of emission of IR radiation by the  $(O_3)_6(H_2O)_{50}$  cluster increases as a result of its interaction with chlorine ions (fig. 6). The ratio of integrated intensities of the  $P(\omega)$  spectrum for  $6O_3 + (H_2O)_{50}$  systems with 0, 2, 4, and 6  $Cl^-$  ions is defined as 1 : 1.34 : 1.16 : 1.07. The amplification of excitement, as a rule, does not result in a more intensive radiation. The maximum of emission spectra of these systems falls to frequency  $945.6 \text{ cm}^{-1}$ .

Thus, as a result of interaction with water cluster,  $Cl^-$  ions can obtain sufficient energy to collide with absorbed ozone molecules and to cause their dissociation. In other words, there can be a destruction of ozone by chlorine near to the surface of the water cluster. Interaction of  $6O_3 + (H_2O)_{50}$  systems with  $Cl^-$  ions causes an increase of integrated intensity of infra-red radiation of emission spectra, and also an essential reduction of similar characteristics of Raman spectrum.

#### V. ESTIMATION OF THE GREENHOUSE EFFECT

Atmospheric water clusters absorb IR radiation going from the Earth, as well as free (not incorporated in clusters) molecules of greenhouse gases create a greenhouse effect. However the quantity of absorption by clusters of radiation is not proportional to the number of molecules forming it. Moreover, clusters absorb energy of IR radiation in quantity comparable, and sometimes even smaller, than that absorbed by free water molecules. (fig. 7). As a result free molecules (before they have been incorporated into cluster) make much stronger absorption of IR radiation (the total intensity  $\sum_i I_i$ ),

than clusters ( $I_{cl}$ ). The difference of values  $\sum_i I_i$  and  $I_{cl}$  is defined as an anti-greenhouse effect of the cluster. This value can be expressed in degrees. The estimation of the anti-greenhouse effect that exists now, created by atmospheric water clusters, can be made as follows.

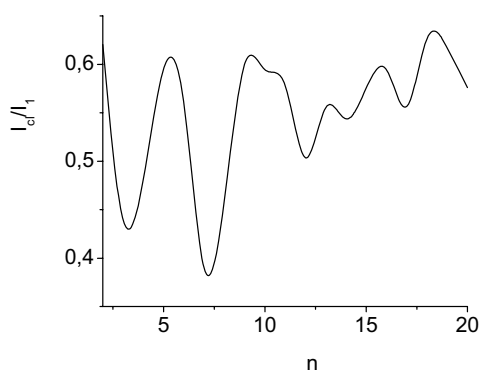


Fig. 7 The relation of integrated intensities of IR radiation absorption by water clusters, formed by  $n$  molecules, to the appropriate characteristic of a free water molecule at average surface humidity of  $11 \text{ g/m}^3$ .

The distribution of the atmospheric moisture at altitude submits to the empirical Ghan dependence [30]:

$$\rho = \rho_0 \cdot 10^{-h/6.3}, \quad (7)$$

where  $\rho_0$  is the humidity at certain altitude (as a rule, direct at the Earth's surface),  $h$  is an altitude in km. On one hand, the formula (7) can be used for calculation of the distribution of water vapor monomer above the Earth's surface, and on another hand – for definition of high-altitude distribution of total moisture in the atmosphere. In the first case, constant  $\rho_0$  is a fraction of water monomers near to the Earth's surface. It can be established by extrapolation of the Boltzmann distribution of clusters on the sizes to the  $i=0$  value. Thus the value determined equals  $\sim 66.3\%$  from known value of humidity ( $\sim 11 \text{ g/m}^3$ ) which at the surface is defined by the number of water monomers and clusters. In the second case value  $\rho_0$  corresponds to the humidity at the altitude of 3 km, established on the basis of spectroscopic measurements [31]. Experimental measurements are executed in the presence of clouds at the altitude from 1 up to 2 km. The spectroscopic sensitive element allows to measure spatially divided profiles of density of moisture both around tropospheric clouds, and inside them. Integration on concentric layers of thickness  $\Delta h$  of the first and second distributions gives value of mass  $M_{vap}$  of vapor monomers and total quantity  $M_{tot}$  of moisture in the atmosphere. The mass of droplets and crystals in the atmosphere was found by the formula

$$M_{drop(cryst)} = \sum_{n=1}^{100} (\rho^{(n)} - \rho_{sv}^{(n)}) V_n,$$

where  $\rho^{(n)}$  and  $\rho_{sv}^{(n)}$  are densities of moisture and saturated water vapor in  $n$  layer thickness of 1 km,  $V_n$  is the volume of a layer.

We consider particles which size exceeds  $0.5 \mu\text{m}$  (the minimal size of a drop observable in clouds) as drops. For separate definition of droplets' and crystals' mass it is necessary to establish temperature intervals where there can be former or later phase. Based on the statistical experimental data we suppose that drops could exist up to temperature  $258 \text{ K}$  ( $-15^\circ \text{C}$ ), and at  $T < 258 \text{ K}$  the cloud consists of ice particles. The  $\rho_{svl}^{(n)}$  density of saturated water vapor over the supercooled water was designed as  $\rho_{sv}^{(n)}$  at the definition of droplets' mass in the atmosphere, and for calculation of crystals' mass the  $\rho_{svc}^{(n)}$  density of saturated water vapor over ice at temperature of  $n$  layer was used. Masses  $M_{drop}$  and  $M_{cryst}$  thus were established. The mass of clusters in the atmosphere was defined as

$$M_{cl} = M_{tot} - M_{vap} - M_{drop} - M_{cryst}.$$

Similarly, through the appropriate distributions, the high-altitude profile of clusters' density was defined. The designed dependences are given in fig. 8. It is visible that the great bulk

of water clusters in the atmosphere settles up to an altitude of 2 km. Overwhelming quantity of drops is concentrated within the limits of the same altitude, and crystals are formed, from the altitude of 3 km. The ratio between quantities of monomer vapor, clusters, drops and crystals looks as 70.0 : 9.2 : 5.9 : 14.9, if total magnitude of the moisture in the atmosphere is 100 %. On average, the integrated intensities of IR radiation absorption of water clusters are lower than the intensity of separate molecules. According to the estimation the number of clusters in the atmosphere at time 2.38 is less than the number of molecules forming them. Created by clusters and corresponding free molecules greenhouse effects are ~ 0.53 and 1.67 K accordingly. Thus, the average temperature of the planet could rise by  $1.67 - 0.53 = 1.14$  K in the absence of clusters, that would result in a significant change of climate. During the last 100 years the average global temperature of the Earth has gone up by 0.6 K [32].

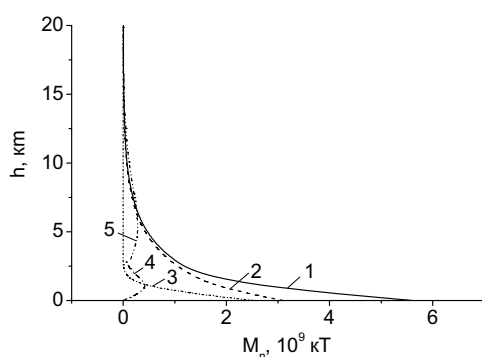


Fig. 8 Contributions to a total mass of the atmosphere moisture: 1 – all moisture, 2 – monomers vapor, 3 – clusters, 4 – droplets, 5 – crystals.

## VI. CONCLUSION

Until recently there is no complete picture of all the factors influencing climate change. The reliability of forecasts depends on an understanding of cycles that result in climate change. For example, space rays represent the main source of ionization of the air. Under the influence of space rays nitrogen oxides are formed, and they destroy the ozone layer of the stratosphere which results in a substantial cooling. As a whole, the warm climate period of the Earth is equivalent to approximately 10 % of the glacial cycle duration which in itself consists of approximately 100 000 years. Hence we are living in a warm climate period that has effectively lasted for 10,000 years. It is expected that in the near future cooling of the planet will take place. The total mass of ozone makes ~  $0.64 \times 10^{-5}$  of the weight of all atmosphere. The depletion of the ozone layer can be connected to other natural phenomena, for example, volcanic eruptions. We can distinguish chloral, nitric and hydrogen cycles of the ozone destruction. Chlorine destroying ozone is not spent at all in this process. At destruction of  $N_2O$  molecules  $N_2$  and  $O_2$  are formed. The basic stocks of hydrogen are concentrated in the nucleus of the planet, and hydrogen through deep fractures emits into the atmosphere. Almost all ozone holes are placed above the seismic zones of the Earth. In the present work we have

shown that atmospheric water clusters are also capable of influencing the climate. Accumulation of  $CO_2$  in the atmosphere has increased since 1900. By 2000 the volumetric concentration of  $CO_2$  has increased by 1.25 times. The anti-greenhouse effect created by clusterization of the atmospheric water vapor limits the growth of global temperature.

Growing concentrations of greenhouse gases increases the thermodynamic disequilibrium of tropical ocean–atmospheric system, and thereby increases the intensity of hurricanes. The total cooling effect of water evaporation from the surface of seas and reservoirs, is 13.4 K. Transition of the part of atmospheric water vapor into clusters causes a decrease of atmospheric temperature by 1.14 K, that is the effect of 8.5% cooling of the heat received during water evaporation. Thus, the content of  $CO_2$  in the atmosphere of the Earth is not an absolute criterion of the efficiency of the greenhouse effect made by this gas which now is estimated at 9.3 K, i.e. constitutes about 19.6% of the effect given by all greenhouse gases. In the absence of reliable thermal protection from the ozone layer of the lower stratosphere and depletion of atomic oxygen in the thermosphere,  $CO_2$  can partially or completely carry out the functions of anti-greenhouse gas.

## REFERENCES

- [1] F. Xie, W. Tian, M.P. Chipperfield, "Radiative effect of ozone change on stratosphere-troposphere exchange", vol. 113, 2008, pp. D00B09, doi: 10.1029/2008JD009829.
- [2] V. Vaida, J.S. Daniels, H.G. Kjaergaard, L.M. Goss, A.F. Tuck, "Atmospheric absorption of near infrared and visible solar radiation by the hydrogen bonded water dimer," *Q.J.R. Meteorol. Soc.*, vol. 127, 2001, pp. 1627–1643.
- [3] K.J. Bignell, "The water vapour infrared continuum," *Q.J.R. Meteorol. Soc.*, vol. 96, 1970, pp. 390–403.
- [4] A.C.L. Lee, "A study of the continuum absorption within the 8-13  $\mu$ m atmospheric window," *Q.J.R. Meteorol. Soc.*, vol. 99, 1973, pp.490–505.
- [5] M.T. Coffey, "Water vapour absorption in 10-12  $\mu$ m atmospheric window," *Q.J.R. Meteorol. Soc.*, vol. 103, 1977, pp. 685–692.
- [6] P.G. Wolynes, R.E. Roberts, "Molecular interpretation of the infrared water vapour continuum", *Applied Optics*, vol. 17, 1978, pp. 1484–1485.
- [7] H.R. Carlon, "Do clusters contribute to the infrared absorption spectrum of water vapor?," *Infrared Phys.*, vol. 19, 1979, pp. 549–557.
- [8] H.A. Gebbie, "Observations of anomalous absorption in the atmosphere", in *Atmospheric water vapor*, A. Deepak, T.D. Wilkerson and L.H. Ruhnke, Ed. New York: Academic Press, 1980, pp. 133–141.
- [9] G.R. Low, H.G. Kjaergaard, "Calculation of OH-stretching band intensities of the water dimer and trimer," *J. Chem. Phys.*, vol. 110, 1999, pp. 9104–9115.
- [10] L.M. Goss, S.W. Sharpe, T.A. Blake, V. Vaida, and J.W. Brault, "Direct absorption spectroscopy of water clusters," *J. Phys. Chem. A*, vol. 103, 1999, pp. 8620–8624.
- [11] J. Barrett, "Greenhouse molecules, their spectra and function in the atmosphere," *Energy & Environment*, vol. 16, 2005, pp. 1037–1045.
- [12] A.Y. Galashev, O.R. Rakhmanova, and V.N. Chukanov, "Absorption and dissipation of infrared radiation by atmospheric water clusters," *Russian Journal of Physical Chemistry*, vol. 79, 2005, pp. 1455–1159.
- [13] O.A. Novruzova, A.A. Galasheva, and A.E. Galashev, "IR spectra of aqueous disperse systems adsorbed atmospheric gases: 1. Nitrogen," *Colloid Journal*, vol. 69, 2007, pp. 474–482.
- [14] O.A. Novruzova, and A.E. Galashev, "Numerical simulation of IR absorption, reflection, and scattering in dispersed water-oxygen media," *High Temperature*, vol. 46, 2008, pp. 60–68.
- [15] O.A. Novruzova, A.A. Galasheva, and A.E. Galashev, "IR spectra of aqueous disperse systems adsorbed atmospheric gases: 2. Argon," *Colloid Journal*, vol. 69, 2007, pp. 483–491.
- [16] L.X. Dang, and T.M. Chang, "Molecular dynamics study of water clusters, liquid and liquid–vapor interface of water with many-body potentials," *J. Chem. Phys.*, vol. 106, 1997, pp. 8149–8159.

- [17] M.A. Spackman, "Atom-atom potentials via electron gas theory," *J. Chem. Phys.*, vol. 85, 1986, pp. 6579–6585.
- [18] M.A. Spackman, "A simple quantitative model of hydrogen bonding," *J. Chem. Phys.*, vol. 85, 1986, pp. 6587–6601.
- [19] J.M. Haile, *Molecular Dynamics Simulation. Elementary Methods*. N.Y.–Chichester–Brisbane–Toronto–Singapore: John Wiley & Sons, Inc., 1992, ch. 4.
- [20] V.N. Koshlyakov, *Zadachi Dinamiki Tverdogo Tela I Prikladnoi Teorii Giroskopov (Problems of Solid Body Dynamics and the Applied Theory of Gyroscopes)*. Moscow: Nauka, 1985, ch. 1.
- [21] R. Sonnenschein "An Improved algorithm for molecular dynamics simulation of rigid molecules," *J. Comp. Phys.*, vol. 59, 1985, pp. 347–350.
- [22] M. Neumann, "The dielectric constant of water. Computer simulations with the MCY potential," *J. Chem. Phys.*, vol. 82, 1985, pp. 5663-5672.
- [23] W.B. Bosma, L.E. Fried, S. J. Mukamel, "Simulation of the intermolecular vibrational spectra of liquid water and water clusters," *J. Chem. Phys.*, vol. 98, 1993, pp. 4413-4421.
- [24] L.D. Landau, and E.M. Lifshitz, *Elektrodinamika Sploshnykh Sred (Electrodynamics of Continuous Media)*, vol. 8, Moscow: Nauka, 1982.
- [25] *Fizicheskaya Entsiklopediya (Physical Encyclopedia)*, vol. 1, A.M. Prokhorov, Ed. Moscow: Sovetskaya entsiklopediya, 1988.
- [26] P.L. Goggin, and C. Carr, "Far infrared spectroscopy and aqueous solutions," in *Water and Aqueous Solutions*, vol. 37, G.W. Neilson, J.E. Enderby, Ed. Bristol: Adam Hilger, 1986, pp. 149-161.
- [27] G. Herzberg, *Molecular Spectra and Molecular Structure: II. Infrared and Raman Spectra of Polyatomic Molecules*. Princeton: Van Nostrand Reinhold, 1945.
- [28] V.I. Kozintsev, M.L. Belov, V.A. Gorodnichev, and Yu.V. Fedotov, *Lazernyi Optiko-akusticheskii Analiz Mnogokomponentnykh Gazovykh Smesey (Laser Optical Acoustic Analysis of Multicomponent Gas Mixtures)*, Moscow: Izd. MG TU im. N.E. Bauman, 2003.
- [29] Ph. Vallee, J. Lafait, M. Ghomi, M. Jouanne, J.F. Morhange, "Raman scattering of water and photoluminescence of pollutants arising from solid-water interaction," *J. Mol. Struct.* vol. 651-653, 2003, pp. 371-379.
- [30] S. J. Ghan, L. R. Leung, R. C. Easter, and H. Abdul-Razzak, "Prediction of cloud droplet number in a general circulation model," *J. Geophys. Res.*, vol. 102(D18), 1997, pp.777–794.
- [31] P.L. Keabian, C.E. Kolb, A. Freedman, "Spectroscopic water vapor sensor for rapid response measurements of humidity in the troposphere," *J. Geophys. Res.* vol. 107(D23), 2002, pp. 4670 (1-14).
- [32] M.M. Halmann, M. Steinberg, *Greenhouse Gas Carbon Dioxide Mitigation. Science and Technology*. Roca Raton, London, New York, Washington: Lewis publishers, 1999, pp. 7–8.